

Structural Evolution Induced Preferential Occupancy of Designated Cation Sites by Eu²⁺ in M₅(Si₃O₉)₂ (M = Sr, Ba, Y, Mn) Phosphors

Yi Wei,^{1,#} Chun Che Lin,^{3,#,*} Zewei Quan,⁴ Maxim S. Molokeev,^{5,6} Victor V. Atuchin,^{7,8,9} Ting-Shan Chan,¹⁰ Yujun Liang,¹ Jun Lin,^{2,*} and Guogang Li,^{1,*}

¹Faculty of Materials Science and Chemistry, China University of Geosciences, Wuhan 430074, P. R. China, Electronic mail:

²State Key Laboratory of Rare Earth Resource Utilization, Changchun Institute of Applied Chemistry, Chinese Academy of Sciences, Changchun 130022, P. R. China

³Condensed Matter and Interfaces, Debye Institute for Nanomaterials Science, Utrecht University, Princetonplein 5, 3584 CC Utrecht, The Netherlands

⁴Department of Chemistry, South University of Science and Technology of China, Shenzhen, Guangdong 518055, P. R. China

⁵Laboratory of Crystal Physics, Kirensky Institute of Physics, Siberian Branch of the Russian Academy of Sciences, Krasnoyarsk 660036, Russia

⁶Department of Physics, Far Eastern State Transport University, Khabarovsk 680021, Russia

⁷Laboratory of Optical Materials and Structures, Institute of Semiconductor Physics, SB RAS, Novosibirsk 630090, Russia

⁸Functional Electronics Laboratory, Tomsk State University, Tomsk 634050, Russia

⁹Laboratory of Semiconductor and Dielectric Materials, Novosibirsk State University, 2 Pirogov Str., Novosibirsk 630090, Russia

¹⁰National Synchrotron Radiation Research Center, Hsinchu 300, Taiwan

#These authors contribution to this work is equal.

Corresponding authors:

*gqli8312@gmail.com

*cclin0530@gmail.com

*jlin@ciac.ac.cn.

EXPERIMENTAL SECTION

Chemicals and Materials. SrCO₃ (\geq 99.99%), BaCO₃ (\geq 99.99%), Y₂O₃ (\geq 99.99%), Eu₂O₃ (\geq 99.99%), and SiO₂ (\geq 99.995%) were purchased from Sigma-Aldrich Corporation. MnCO₃ (99.99%) were purchased from Sinopharm Chemical Reagent Co., Ltd. (Shanghai). All of the initial chemicals were used without further purification. Alumina crucibles were used to sinter the phosphor samples.

Preparation. A series of Sr_{2.97-x}Ba_xEu_{0.03}Y₂(Si₃O₉)₂ ($x = 0\text{--}1.59$) and Sr_{2.97-y}Mn_yEu_{0.03}Y₂(Si₃O₉)₂ ($y = 0\text{--}0.63$) compounds were prepared by a conventional high-temperature solid state reaction. Stoichiometric amounts of SrCO₃, BaCO₃, MnCO₃, Y₂O₃, Eu₂O₃, and SiO₂ were thoroughly mixed and pestled in an agate mortar for 1 h. Then, the powder mixtures were placed in alumina crucibles and sintered in a horizontal tube furnace at 1150°C–1250°C for 6 h with the reducing atmosphere of H₂ (8%) and N₂ (92%) atmosphere. After the furnace being slowly cooled to room temperature, the sintered products were grinded again, generating the final phosphor powders.

Characterization. Finely ground powders were used in all measurements. The phase purity of all samples were analyzed using X-ray diffraction (XRD) obtained by a D8 Focus diffractometer (Bruker, Kalsruhe, Germany) at the scanning rate of 1° min⁻¹ in the 2θ range from 5° to 120°, and the counting time was 5 s per step with Ni-filtered Cu K α radiation ($\lambda = 0.15406$ nm). The XRD Rietveld profile refinements of the structural models and texture analysis were performed with the use of General Structure Analysis System (GSAS) and TOPAS 4.2 software. [Bruker AXS *TOPAS V4: General profile and structure analysis software for powder diffraction data. – User's Manual*, Bruker AXS, Karlsruhe, Germany, 2008.] The starting model was built with crystallographic data taken from Tyutyunnik *et al.* [Tyutyunnik, A. P.; Leonidov, I. I.; Surat, L. L.; Berger I. F.; Zubkov, V. G. *J. Solid State Chem.* **2013**, *197*, 447–455.] Chemical formulas obtained from refinements were close to suggested formula. As far as chemical compositions of compounds were proved by coupled plasma optical emission spectrometer (ICP-OES, ICAP 6300, Thermal Scientific), it was decided to use penalty on sum of occupancies according to chemical formula during refinement.

The photoluminescence measurements were recorded with a Fluoromax-4P spectrophotometer (Horiba Jobin Yvon, New Jersey, U.S.A.) equipped with a 450 W xenon lamp as the excitation source. Both excitation and emission spectra were set up to be 1.0 nm with the width of the monochromator slits adjusted to 0.50 nm. The thermal stability of luminescence of phosphor materials were measured by Fluoromax-4P spectrometer connected a heating equipment (TAP-02). The photoluminescence decay curves were obtained from a Lecroy Wave Runner 6100 Digital Oscilloscope (1 GHz) using a tunable laser (pulse width = 4 ns, gate = 50 ns) as the excitation (Continuum Sunlite OPO). All the measurements were performed at room temperature (RT).

Table S1. Main parameters of processing and refinement of the $\text{Sr}_{2.97-x}\text{Ba}_x\text{Eu}_{0.03}\text{Y}_2(\text{Si}_3\text{O}_9)_2$ ($x = 0\text{--}1.59$) samples

x	Phase, Weight	Space group	Cell parameters, \AA	Cell volume, \AA^3	$R_{wp}, R_p,$ $R_{exp}, \%, \chi^2$	$R_B, \%$
			$a = 13.5105(2)$			
0	Phase1, 100%	$C2/c$	$b = 7.9815(1)$ $c = 14.8222(3)$ $\beta = 90.097(1)$ $a = 13.5089(3)$	1598.35(5)	9.30, 6.32, 2.96, 3.14	4.23
0.06	Phase1, 100%	$C2/c$	$b = 7.9920(2)$ $c = 14.8055(4)$ $\beta = 90.120(1)$ $a = 13.5112(3)$	1598.45(7)	5.91, 4.35, 2.54, 2.33	3.17
0.09	Phase1, 100%	$C2/c$	$b = 7.9992(2)$ $c = 14.7931(4)$ $\beta = 90.147(2)$ $a = 13.5182(5)$	1598.80(7)	6.17, 4.39, 2.48, 2.49	3.01
	Phase1, 57 (9)%	$C2/c$	$b = 8.0035(3)$ $c = 14.7902(6)$ $\beta = 90.180(2)$ $a = 13.4440(9)$	1600.2(1)		4.48
0.12	Phase2, 43 (9)%	$C2/c$	$b = 8.2800(6)$ $c = 13.792(1)$ $\beta = 93.096(6)$ $a = 13.5170(4)$	1533.0(2)		2.59
	Phase1, 40 (1)%	$C2/c$	$b = 8.0031(2)$ $c = 14.7803(4)$ $\beta = 90.199(2)$ $a = 13.4365(4)$	1598.90(7)		2.79
0.15	Phase2, 60 (1)%	$C2/c$	$b = 8.2885(2)$ $c = 13.7846(5)$ $\beta = 93.114(2)$ $a = 13.5159(5)$	1532.91(8)	4.58, 3.38, 2.50, 1.83	1.69
	Phase1, 21.6 (5)%	$C2/c$	$b = 8.0031(3)$ $c = 14.7734(6)$ $\beta = 90.224(3)$ $a = 13.4362(3)$	1598.0(1)		1.98
0.18	Phase2, 78.4 (5)%	$C2/c$	$b = 8.2883(2)$ $c = 13.7795(3)$ $\beta = 93.118(1)$	1532.26(5)	4.01, 2.99, 2.44, 1.65	1.70

<i>x</i>	Phase, Weight	Space group	Cell parameters, Å	Cell volume, Å ³	<i>R</i> _{wp} , <i>R</i> _p , <i>R</i> _{exp} , %, χ^2	<i>R</i> _B , %
0.21	Phase2, 100%	<i>C</i> 2/ <i>c</i>	<i>a</i> = 13.4371(3) <i>b</i> = 8.2893(2) <i>c</i> = 13.7772(3) β = 93.105(1) <i>a</i> = 13.4423(3)	1532.30(6)	4.95, 3.59, 2.47, 2.01	1.90
0.27	Phase2, 100%	<i>C</i> 2/ <i>c</i>	<i>b</i> = 8.2927(2) <i>c</i> = 13.7814(3) β = 93.0797(9) <i>a</i> = 13.4461(2)	1534.03(6)	4.27, 3.18, 2.43, 1.76	1.78
0.33	Phase2, 100%	<i>C</i> 2/ <i>c</i>	<i>b</i> = 8.2948(1) <i>c</i> = 13.7824(2) β = 93.0519(9) <i>a</i> = 13.4516(2)	1535.00(4)	6.63, 4.48, 2.96, 2.24	2.88
0.39	Phase2, 100%	<i>C</i> 2/ <i>c</i>	<i>b</i> = 8.2988(2) <i>c</i> = 13.7850(3) β = 93.0194(9) <i>a</i> = 13.4627(2)	1536.72(5)	6.58, 4.46, 3.00, 2.20	2.86
0.51	Phase2, 100%	<i>C</i> 2/ <i>c</i>	<i>b</i> = 8.3059(2) <i>c</i> = 13.7899(3) β = 92.969 (1) <i>a</i> = 13.4903 (3)	1539.91(5)	6.87, 4.63, 3.03, 2.27	3.35
0.87	Phase2, 100%	<i>C</i> 2/ <i>c</i>	<i>b</i> = 8.3250 (2) <i>c</i> = 13.777 (1) β = 92.777 (1) <i>a</i> = 13.5085 (3)	1548.42 (6)	7.21, 4.82, 3.09, 2.33	3.30
1.11	Phase2, 100%	<i>C</i> 2/ <i>c</i>	<i>b</i> = 8.3388 (2) <i>c</i> = 13.8142 (3) β = 92.649 (1) <i>a</i> = 13.5245 (3)	1554.43 (6)	6.92, 4.57, 3.13, 2.21	3.10
1.35	Phase2, 100%	<i>C</i> 2/ <i>c</i>	<i>b</i> = 8.3504 (2) <i>c</i> = 13.8220 (3) β = 92.541 (1) <i>a</i> = 13.5416 (3)	1559.44 (6)	6.91, 4.51, 3.18, 2.17	2.92
1.59	Phase2, 100%	<i>C</i> 2/ <i>c</i>	<i>b</i> = 8.3630 (2) <i>c</i> = 13.8329 (3) β = 92.442 (1)	1565.16 (6)	4.95, 3.59, 2.67, 1.85	2.51

Table S2. The identification of chemical composition of three representative $\text{Sr}_{2.97-x}\text{Ba}_x\text{Eu}_{0.03}\text{Y}_2(\text{Si}_3\text{O}_9)_2$ ($x = 0.06, 0.15, 1.59$) samples

Content x	Sr	Ba	Y	Eu	Theoretical	Experimental
	/ppm	/ppm	/ppm	/ppm	chemical formula	chemical formula
$x = 0.06$	266800	13410	193400	4107	$\text{Sr}_{2.91}\text{Ba}_{0.03}\text{Eu}_{0.03}\text{Y}_2(\text{Si}_3\text{O}_9)_2$	$\text{Sr}_{2.83}\text{Ba}_{0.08}\text{Eu}_{0.024}\text{Y}_{1.95}(\text{Si}_3\text{O}_9)_2$
$x = 0.15$	260000	190400	25960	4413	$\text{Sr}_{2.82}\text{Ba}_{0.15}\text{Eu}_{0.03}\text{Y}_2(\text{Si}_3\text{O}_9)_2$	$\text{Sr}_{2.66}\text{Ba}_{0.17}\text{Eu}_{0.026}\text{Y}_{1.92}(\text{Si}_3\text{O}_9)_2$
$x = 1.59$	168800	246600	293100	5274	$\text{Sr}_{1.38}\text{Ba}_{1.59}\text{Eu}_{0.03}\text{Y}_2(\text{Si}_3\text{O}_9)_2$	$\text{Sr}_{1.73}\text{Ba}_{1.91}\text{Eu}_{0.031}\text{Y}_{2.48}(\text{Si}_3\text{O}_9)_2$

Table S3. The CIE color coordinate values and emission peaks of $\text{Sr}_{2.97-x}\text{Ba}_x\text{Eu}_{0.03}\text{Y}_2(\text{Si}_3\text{O}_9)_2$ ($x = 0-1.59$) samples

$\text{Sr}_{2.97-x}\text{Ba}_x\text{Eu}_{0.03}\text{Y}_2(\text{Si}_3\text{O}_9)_2$	CIE x	CIE y	Emission peak / nm
1, $x = 0$	0.168	0.258	474
2, $x = 0.06$	0.162	0.239	470
3, $x = 0.09$	0.161	0.205	468
4, $x = 0.12$	0.157	0.139	451
5, $x = 0.15$	0.156	0.105	442
6, $x = 0.18$	0.157	0.085	440
7, $x = 0.21$	0.157	0.073	437
8, $x = 0.33$	0.157	0.072	438
9, $x = 0.51$	0.157	0.069	436
10, $x = 1.11$	0.158	0.064	435
11, $x = 1.59$	0.160	0.061	432

Table S4. Structural parameters of refinement of the XRD data of $\text{Sr}_{2.97-y}\text{Mn}_y\text{Eu}_{0.03}\text{Y}_2(\text{Si}_3\text{O}_9)_2$ ($y = 0\text{--}0.63$) samples

y	0	0.03	0.15	0.27	0.48	0.51	0.63
Sp.Gr.	$C2/c$						
$a, \text{\AA}$	13.5102(2)	13.5164(3)	13.5144(2)	13.5125(2)	13.5082(4)	13.5068(5)	13.5069(6)
$b, \text{\AA}$	7.9812(1)	7.9826(2)	7.9745(1)	7.9712(1)	7.9659(2)	7.9657(3)	7.9630(4)
$c, \text{\AA}$	14.8217(3)	14.8239(3)	14.8283(3)	14.8257(3)	14.8227(4)	14.8221(6)	14.8227(7)
$\alpha = \gamma$	90	90	90	90	90	90	90
$\beta, {}^\circ$	90.097(1)	90.115(1)	90.121(1)	90.126(9)	90.123(8)	90.115(2)	90.131(3)
$V, \text{\AA}^3$	1598.18(5)	1599.43(6)	1598.04(5)	1596.89(5)	1595.00(8)	1594.7(1)	1594.3(1)
Z	1	1	1	1	1	1	1
$R_{wp}, \%$	9.10	10.40	8.87	5.31	7.37	8.75	16.33
$R_p, \%$	6.16	7.00	6.13	3.89	4.67	5.15	9.42
$R_{exp}, \%$	2.96	2.88	2.86	2.37	2.36	2.33	2.93
χ^2	3.08	3.61	3.10	2.24	3.13	3.77	5.57
$R_B, \%$	4.15	6.04	5.33	2.76	2.60	2.66	5.34

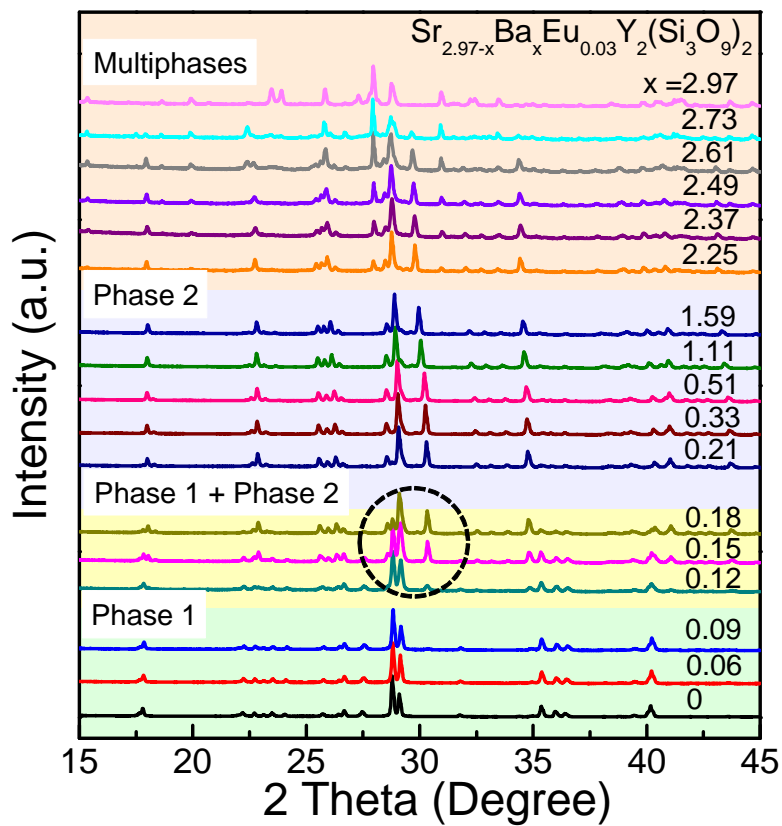


Figure S1. XRD patterns of $\text{Sr}_{2.97-x}\text{Ba}_x\text{Eu}_{0.03}\text{Y}_2(\text{Si}_3\text{O}_9)_2$ (Phase 1, $x = 0\text{--}0.09$; Phase 2, $x = 0.18\text{--}1.59$; Phase 1 + Phase 2, $0.09 < x < 0.18$, $x = 0.12\text{--}0.09$; Multiphases, $x > 1.59$). The multiphased mixtures including BaSi_2O_5 , $\text{Ba}_5\text{Si}_8\text{O}_{21}$, $\text{BaY}_2\text{Si}_3\text{O}_{10}$ foreign phases.

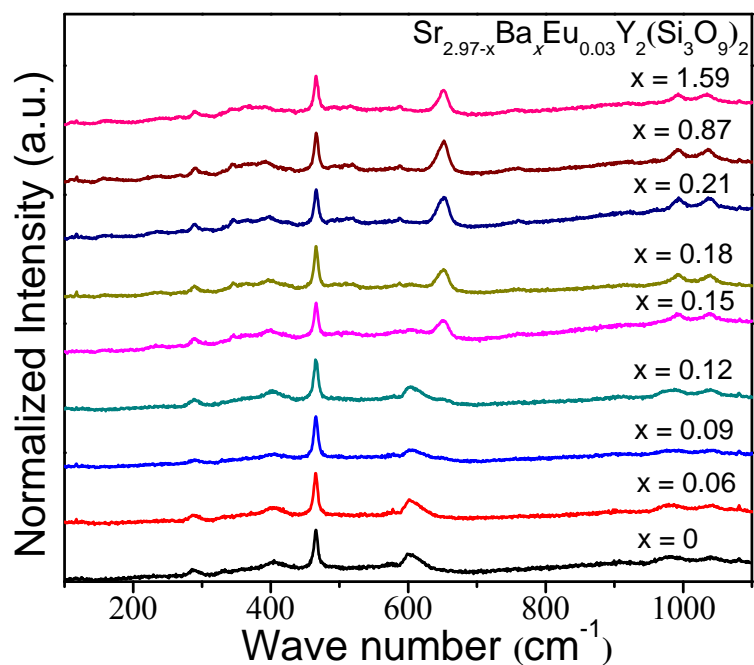


Figure S2. Raman spectra of $\text{Sr}_{2.97-x}\text{Ba}_x\text{Eu}_{0.03}\text{Y}_2(\text{Si}_3\text{O}_9)_2$ ($x = 0\text{--}1.59$) samples.

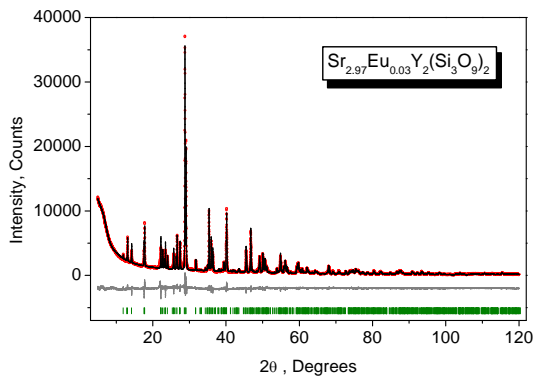


Figure S3

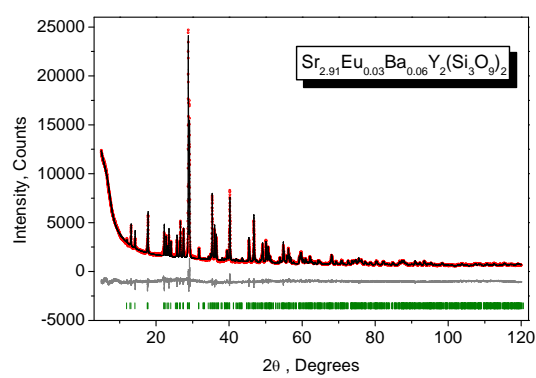


Figure S4

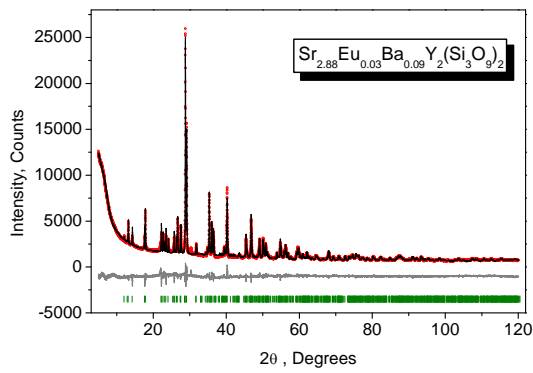


Figure S5

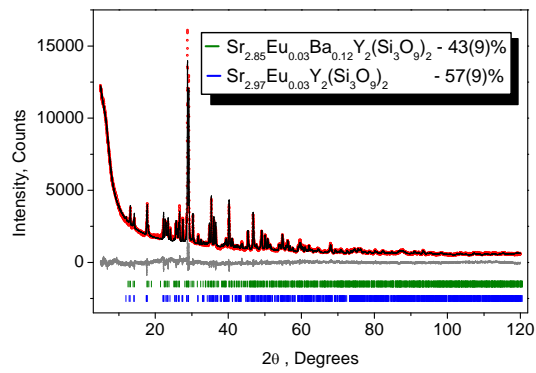


Figure S6

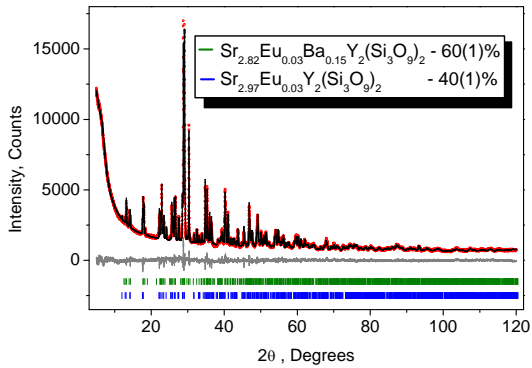


Figure S7

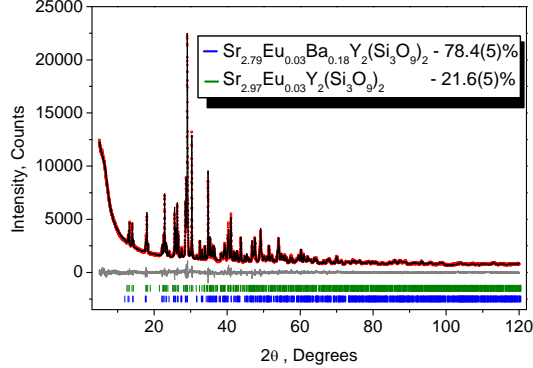


Figure S8

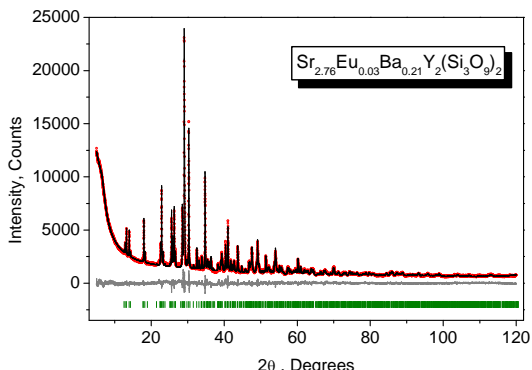


Figure S9

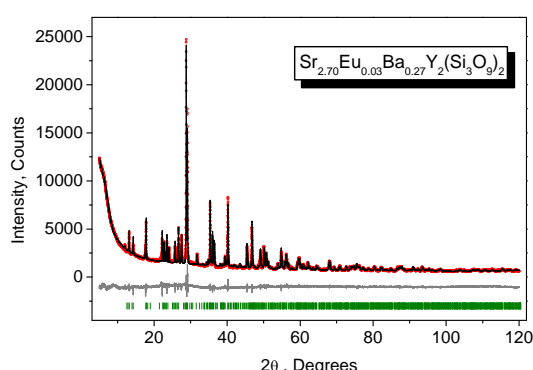


Figure S10

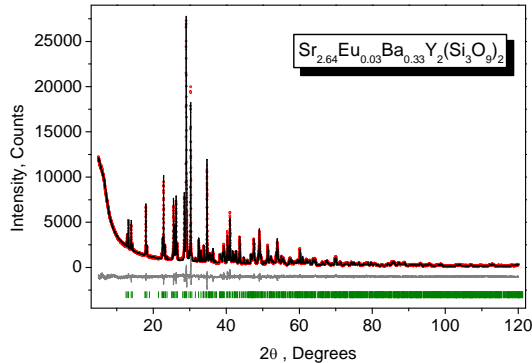


Figure S11

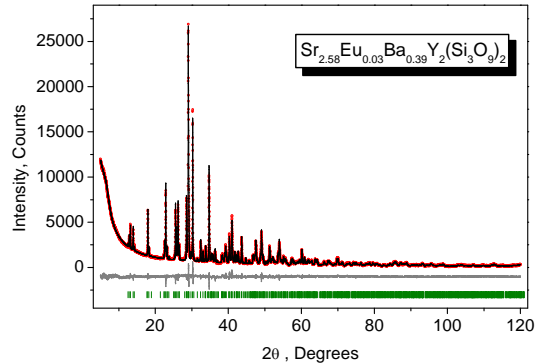


Figure S12

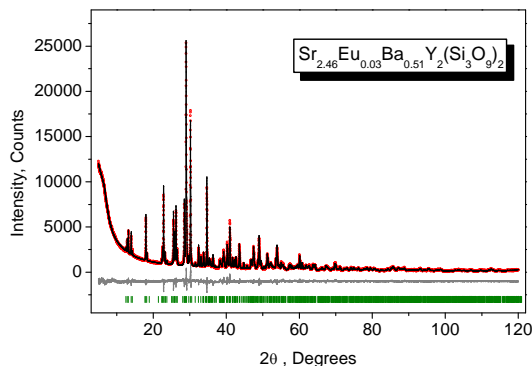


Figure S13

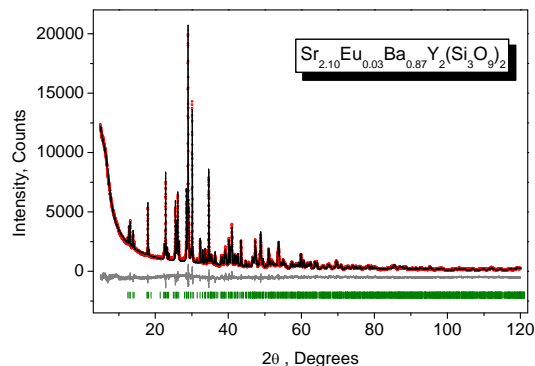


Figure S14

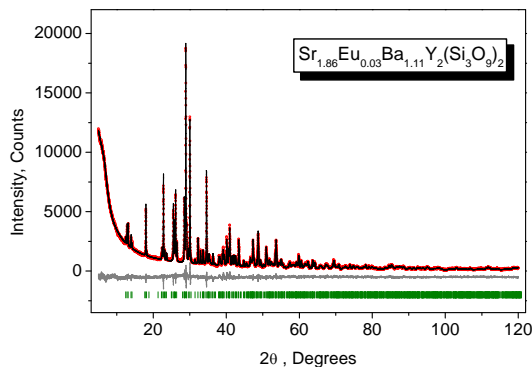


Figure S15

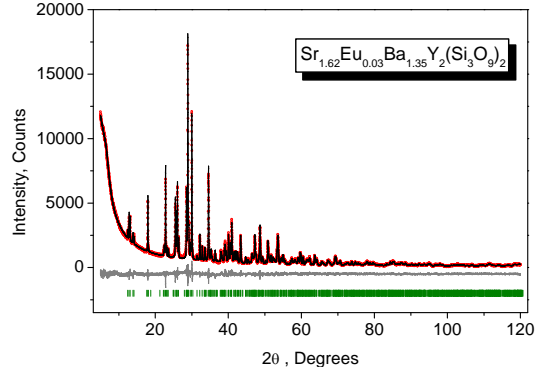


Figure S16

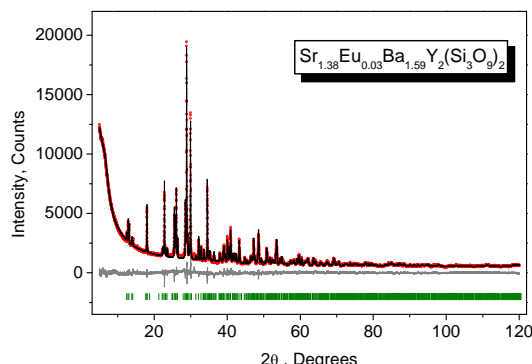


Figure S17

Figure S3-S17. The Rietveld refinement for the XRD pattern of the $\text{Sr}_{2.97-x}\text{Ba}_x\text{Eu}_{0.03}\text{Y}_2(\text{Si}_3\text{O}_9)_2$ ($x = 0\text{--}1.59$) samples (red circles, black line, gray line, green/blue vertical lines are calculation, experiment, difference patterns and Bragg positions, respectively).

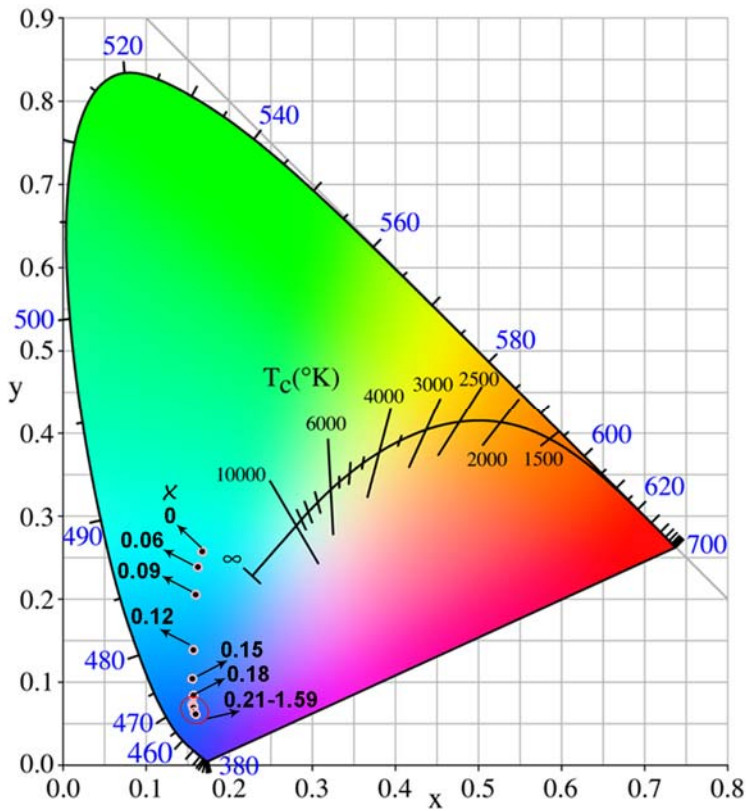


Figure S18 The CIE color coordinate diagram of $\text{Sr}_{2.97-x}\text{Ba}_x\text{Eu}_{0.03}\text{Y}_2(\text{Si}_3\text{O}_9)_2$ ($x = 0\text{--}1.59$) with x (Ba).

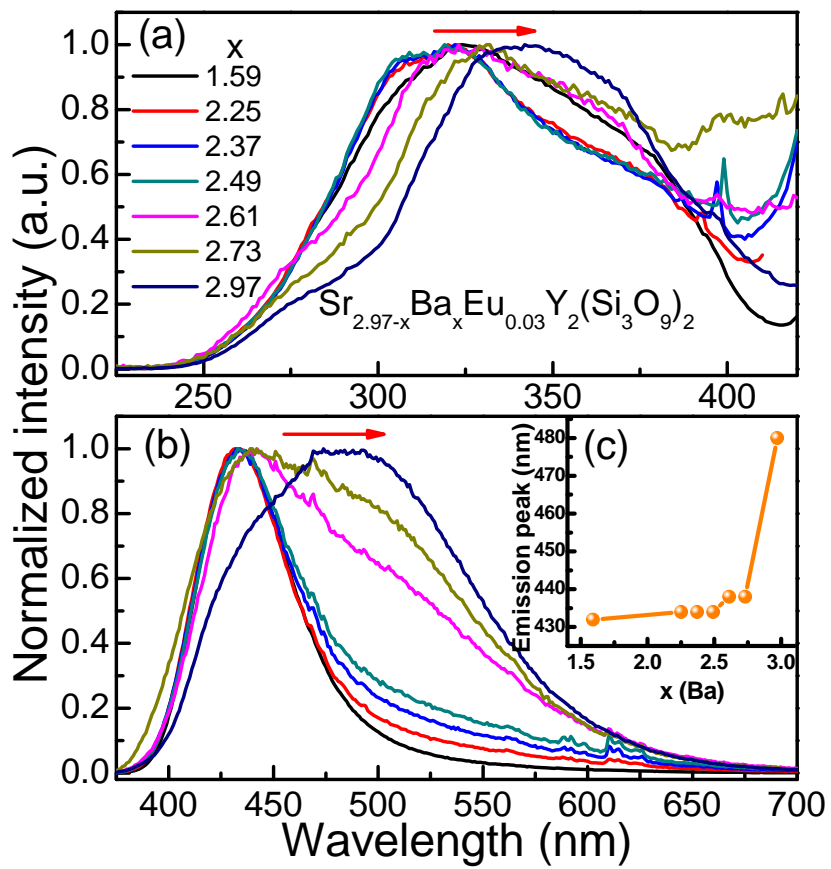


Figure S19 (a) Photoluminescence excitation (PLE) and (b) photoluminescence emission (PL) spectra of $\text{Sr}_{2.97-x}\text{Ba}_x\text{Eu}_{0.03}\text{Y}_2(\text{Si}_3\text{O}_9)_2$ ($x = 1.59\text{--}2.97$), which are obtained by monitoring at max emission and excitation wavelengths, respectively. (c) The emission peaks of $\text{Sr}_{2.97-x}\text{Ba}_x\text{Eu}_{0.03}\text{Y}_2(\text{Si}_3\text{O}_9)_2$ ($x = 1.59\text{--}2.97$) with x (Ba).

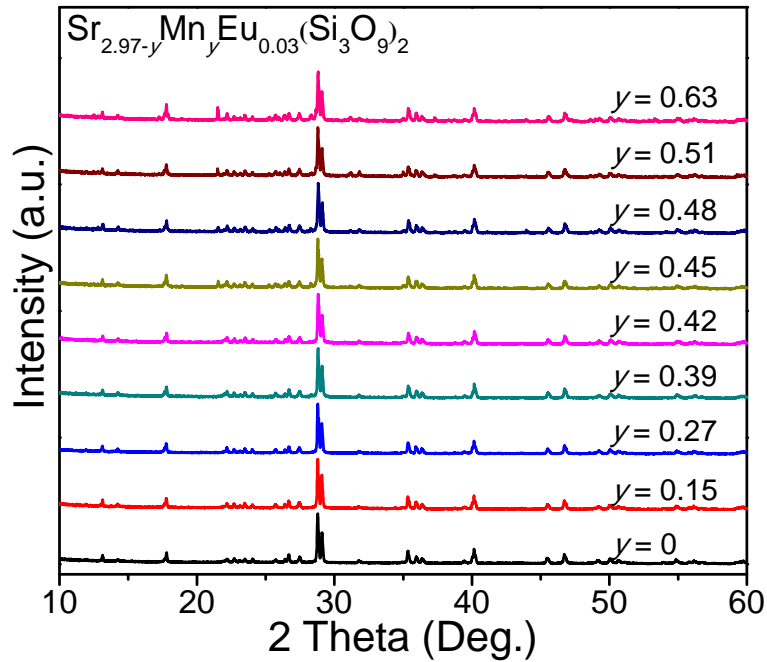


Figure S20. The XRD patterns of $\text{Sr}_{2.97-y}\text{Mn}_y\text{Eu}_{0.03}(\text{Si}_3\text{O}_9)_2$ ($y = 0\text{--}0.63$) samples. Obviously, the diffraction peaks of $\text{Sr}_{2.97-y}\text{Mn}_y\text{Eu}_{0.03}(\text{Si}_3\text{O}_9)_2$ ($y = 0\text{--}0.63$) samples shift to larger-angles direction with the increase of Mn²⁺ concentration, which is in agreement with Vegard rule, implying the formation of $\text{Sr}_{2.97-y}\text{Mn}_y\text{Eu}_{0.03}(\text{Si}_3\text{O}_9)_2$ ($y = 0\text{--}0.63$) solid solutions.

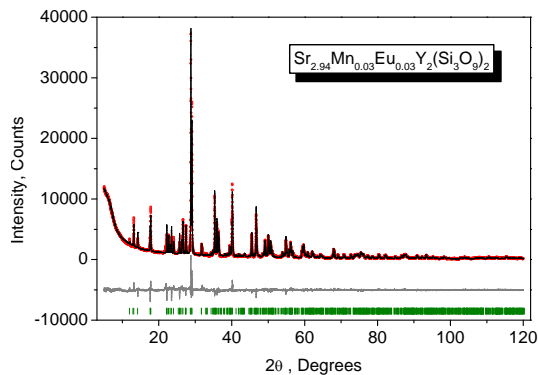


Figure S21

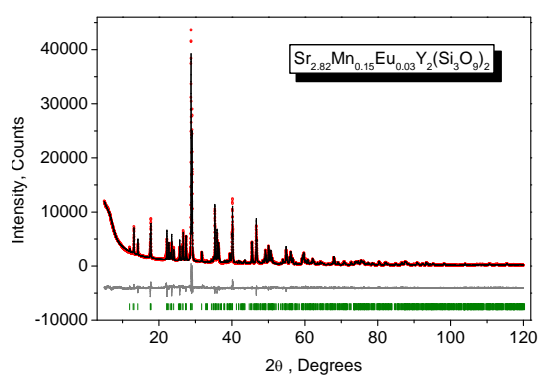


Figure S22

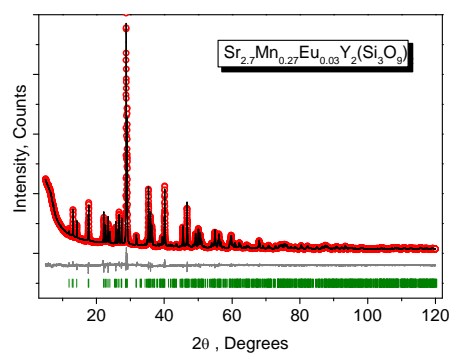


Figure S23

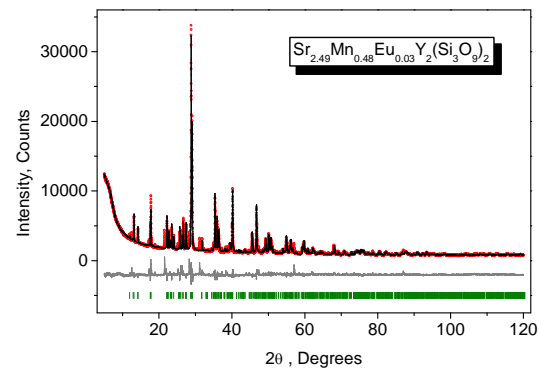


Figure S24

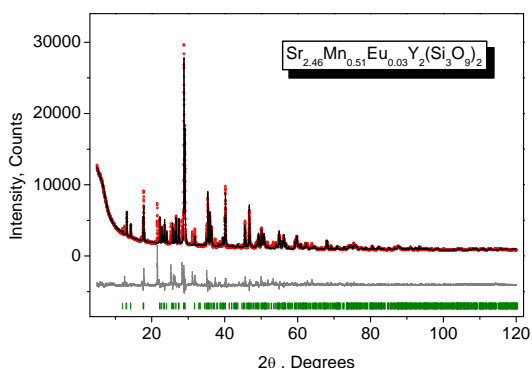


Figure S25

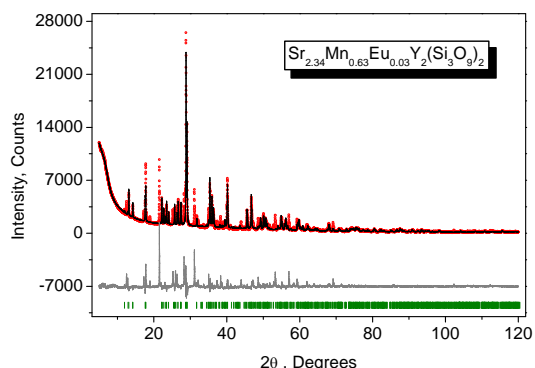


Figure S26

Figure S21-S26. The Rietveld refinement for the XRD pattern of the $\text{Sr}_{2.97-y}\text{Mn}_y\text{Eu}_{0.03}\text{Y}_2(\text{Si}_3\text{O}_9)_2$ ($y = 0.03\text{--}0.63$) samples (red circles, black line, gray line, green vertical lines are calculation, experiment, difference patterns and Bragg positions, respectively).

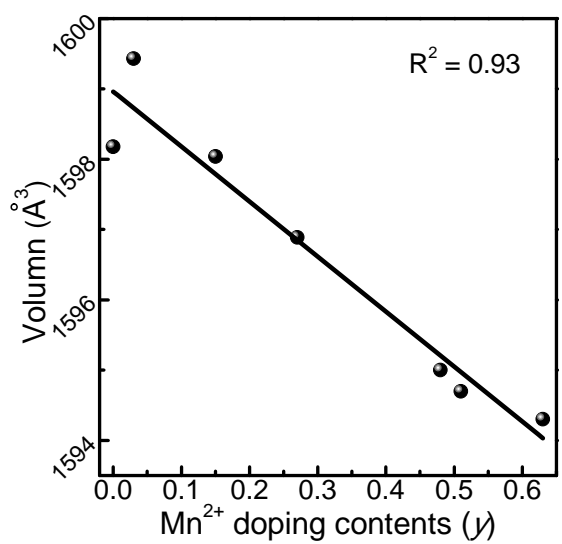


Figure S27. Cell volume (V) as a function of Mn^{2+} doping contents (y) in Mn series.